

FULL PAPER

3D Model of the Acetylcholinesterase Catalytic Cavity Probed by Stereospecific Organophosphorous Inhibitors

Philippe P. Bernard¹, Dmitri B. Kireev¹, Jacques R. Chrétien¹, Pierre-Louis Fortier², and Lucien Coppet²

¹Laboratory of Chemometrics, University of Orléans, BP 6759, F-45067 Orléans, France. Tel: +33-238417076; Fax: +33-238417221. E-Mail: Jacques.Chretien@univ-orleans.fr

²Centre d'Etudes du Bouchet, D.G.A., B.P. N° 3, F-91710 Vert le Petit, France.

Received: 21 April 1998 / Accepted: 28 September 1998 / Published: 21 October 1998

Abstract Automated docking was performed for stereospecific and quasi-irreversible organophosphorous acetylcholinesterase (AChE) inhibitors. Twelve chiral inhibitor structures, corresponding to six enantiomeric pairs, each with a phosphorus atom as a stereocentre, were docked to the crystal structure of mouse AChE. This study gives evidence that in inhibitors with different aromatic and cationic leaving groups these groups are oriented towards the entry of the active site, as recently suggested by Hosea *et al* [1] for inhibitors with a thiocholine leaving group. The results of the docking were used to establish a three dimensional model of the volume sterically available to the inhibitors within the AChE active site.

Keywords Irreversible AChE inhibitors, Organophosphorous compounds, Docking

Introduction

The function of AChE is to recycle acetylcholine (ACh) by its hydrolysis at cholinergic synapses in order to restore the membrane potential after propagation of a nerve impulse [2]. AChE is a target enzyme for biologically active compounds ranging from anti-Alzheimer disease agents [3], acting as reversible inhibitors [4] to pesticides [5] and warfare agents, acting as reversible or irreversible inhibitors [6].

A large quantity of structure-activity data is currently available about the quasi-irreversible organophosphorous inhibitors that phosphorylate AChE at its catalytic site [7-10]. However, no general and reliable approach to predict-

ing the AChE inhibitory activity of new organophosphorous inhibitors has yet been established. The known quantitative structure-activity relationships (QSAR) are limited to homogeneous series with structural variation at a single substitution site [11, 12]. The basic reason for the lack of predictive models of the inhibitory activity is that AChE inhibitors bind themselves virtually inside the enzyme and not on its surface. Hence, each point of an inhibitor's surface interacts with the enzyme and even small structural changes distant from the reacting functional group may cause very important changes in activity. This makes it impossible to derive a predictive model for the AChE inhibitory activity without a detailed understanding of how an inhibitor binds to the enzyme and what the structure of the enzyme's binding cavity is.

A first attempt of giving a detailed description of the binding of organophosphorous inhibitors to AChE was made

Correspondence to: J.R. Chrétien

by Järv [13] who started from the analysis of structure-activity data. He also based his approach on existing models of the substrate-enzyme interactions including interactions at the "catalytic" site [14] and "peripheral" site [15]. The "catalytic" site was in turn subdivided into the "esterasic" site, comprising among others the reacting serine residue, and the "anionic" site, whose tryptophan attracts the quaternary nitrogen of the choline fragment of ACh. Järv presented the catalytic site as a combination of distinct pockets, each of which receives a particular inhibitor's substituent (e.g. charged leaving group, non-charged leaving group, alkyl moiety). This discrete model was able to explain many features of the organophosphorous ligand action. For example, after analysing the ground state and transition state geometries of tetrahedral carbon and pentavalent phosphorus, Järv stated that the pocket receiving the leaving group of substrates is different from the one receiving the leaving group of inhibitors.

More recent studies added new pockets to the "pocket" model, which made it even more fuzzy. Hosea *et al* [1] recently suggested that in mouse AChE the cationic organophosphonate leaving group binds to Asp 74, thus reinforcing Järv's hypothesis and "creating" a new pocket, an anionic one. Then, Ordentlich *et al* [16] showed that the *p*-nitrophenyl leaving group of paraoxon in human AChE interacts with yet another pocket, an "alkoxy" one formed by residues Trp86, Tyr337 and Phe338.

The increasing complication of the "pocket" model prompted us to investigate a new approach to the problem. The present availability of the three dimensional structure of AChE [17, 18] with site-specific mutagenesis data [1, 16, 19-21] and structure activity data [8-10], allows us to construct a new three-dimensional model for the cavity that binds

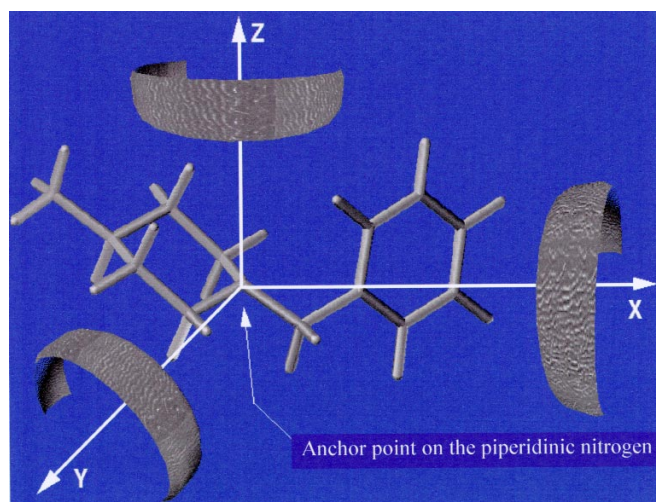


Figure 1 The automated docking procedure. The piperidinic nitrogen was projected on place of the edrophonium's quaternary nitrogen. This position was used as an anchor point for rotations of the studied molecules studied around X, Y and Z axes. A conformational search was performed at each molecule's orientation

the organophosphorous inhibitors. In the present study, we have applied an automated docking technique [22] to a series of six organophosphorous inhibitors, each with a stereocentre at the phosphorous atom in both *R* and *S* absolute configurations, in order to probe what space is available for these compounds inside the enzyme. Firstly, this study aims to delineate a spatial model of AChE catalytic cavity. The second issue concerns the structures of the inhibitor-enzyme complexes. These may be used as an input for following 3D QSAR analyses.

The automated docking we developed can serve as a complement to earlier experimental [1, 16-21] and modelling [1, 16, 23] studies on the inhibition of AChE by organophosphorous ligands. This method is different from manual docking or molecular dynamics in that the space available within the enzyme is systematically probed by the bulky compounds in every possible conformation and orientation, so that every low energy ligand-enzyme complex structure will be found. The agglomerate of the ligands extracted from all the low energy complexes obtained represents a mould of the enzyme's cavity.

Methods

Enzyme structure

The AChE crystal structures were obtained from Brookhaven Protein Data Bank (PDB). Currently, PDB has two types of 3D AChE structures available: (i) AChE from the *Torpedo californica* electric organ (PDB code: 1ACE [17]) further referred to as TACHe and (ii) AChE from mouse (PDB code: 1MAH [18]) further referred to as MACHe. The inhibitory activity data used in the present study were measured on the AChE from bovine erythrocytes whose three dimensional structure is currently not available.

We studied the homology between the bovine and available acetylcholinesterases in order to find out which available structure better fits the bovine enzyme. To carry out this comparison, we aligned MACHe, TACHe and the bovine AChE. At this step it was found that MACHe and bovine AChE are easily superimposable. Superimposing catalytic Ser203 of these two proteins aligns almost the entire protein sequence (583 residues). A one by one comparison of these 583 residues revealed 44 differing residues.

The difference between TACHe and bovine AChE is much more significant. TACHe can be divided into three regions, each of which can be aligned with the corresponding region in bovine AChE. The links between these regions are different in both enzymes. In total, within the three superimposable regions, which number 536 residues, the one by one comparison of residues revealed 232 differing residues. Two of the differing residues, Phe330→Tyr337 and Ile439→Pro446, are located close to the catalytic site and may interact with the inhibitors. It was recently shown that even rather insignificant mutations such as F295Y or E202Q can cause a sig-

nificant change in the enzyme activity [1, 21]. Thus taking MACHe as the object of our docking study decreased the risk of having non-pertinent results, since this enzyme has no differing residues at the catalytic site as compared to the bovine one.

To make its structure suitable for further modelling, hydrogen atoms were added to the original PDB structure using the BIOPOLYMER module of Sybyl [24]. Then the geometry of the protein was optimised using the AMBER force field [25].

Our further intention was to exploit known crystal structures of ligand-enzyme complexes as a source of geometric constraints for the automated docking procedure. However, crystallised ligand-enzyme complexes are only available for TACHe whose structures of TACHe complexed with decamethonium, edrophonium and THA have recently been reported [26]. Two of the three inhibitors, decamethonium and edrophonium, possess a quaternary nitrogen atom binding at the anionic site interacting with residue Trp84 by means of π -cation interactions [27]. When docking ACh, it appeared suitable to locate its quaternary nitrogen in the same position as the decamethonium's nitrogen or the edrophonium's one. Hence, the position of this atom can be used as a required geometric constraint for ACh. We then projected the quaternary nitrogen from TACHe onto MACHe as described in Bernard *et al* [22].

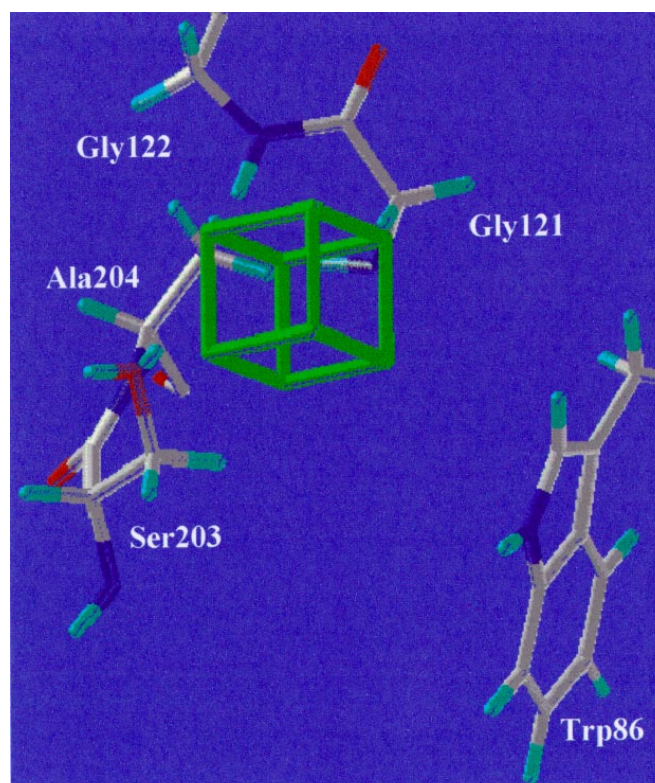


Figure 2 The green cube illustrates the region scanned by the phosphoryl group within the catalytic site of MACHe

Ligands

The compounds used in this paper are listed in Table 1 with their AChE inhibitory activities [8]*. The enzymatic measures for these stereochemical organophosphorous compounds are expressed in the form of inhibition constants (K_i). As the experiments were performed at pH=7.7, the compounds having a basic nitrogen atom were considered in their protonated forms. For compounds **5**, **6**, the K_i values were not available. However, we selected these inhibitors since they are extremely toxic in rats. Compound **5** has a LD_{50} value of 66 $\mu\text{g}\cdot\text{kg}^{-1}$ and that for compound **6** is 16.8 $\mu\text{g}\cdot\text{kg}^{-1}$. This high toxicity indicates that the inhibitory potency of these compounds should also be high. Additionally, compound **5** simultaneously possesses a charged group, a bulky aromatic group, and a bulky alkyl group, which together make it an ideal probe for the AChE binding cavity.

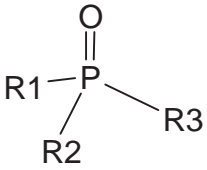
Each of the ligands was modelled using Sybyl 6.3 on a Silicon Graphics *INDY R5000* workstation. The starting conformations were optimised by a molecular mechanics algorithm using the Tripos Force Field [28]. The lowest energy conformations were found by means of the SYBYL/SEARCH option and then used as initial conformations for docking.

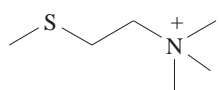
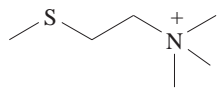
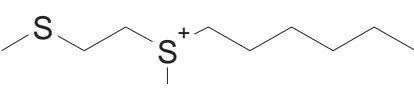
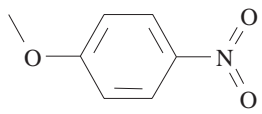
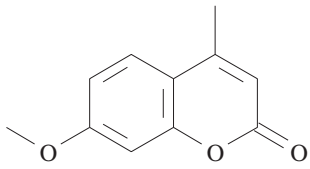
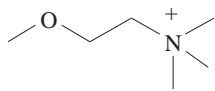
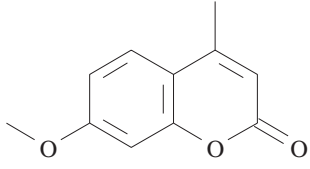
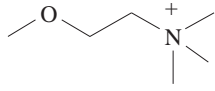
Ligand-enzyme docking

A three step docking strategy was applied in order to optimise the use of available structural constraints, thus minimising the computational time. The first step was to dock ACh with its quaternary nitrogen anchored in the position of the edrophonium's quaternary nitrogen (see the *Enzyme Structure* section for details). The automated docking procedure consisted reorienting of the inhibitor inside the fixed enzyme while simultaneously twisting all rotatable bonds. The inhibitor was reoriented relative to three coordinate axes, as shown in figure 1, with an angle step of 30°. Sybyl's SYSTEMATIC SEARCH was performed for each orientation of the inhibitor. The angle step for the search was 30° and the energy of the entire inhibitor-enzyme complex was calculated at each step. The position of the ACh carbonyl group resulting from this docking analysis then served as the centre of the region probed for placing the inhibitors' phosphoryl group.

The purpose of the second step was to find an appropriate position for the phosphoryl group. At this step not only did we reorient the inhibitor and twist the rotatable bonds but also translated it within the enzyme cavity. The systematic translation consisted moving the phosphorous atom from one lattice intersection to another. The period of the lattice was 0.5 Å and it was limited by a cube with a 2 Å edge. This resulted in 125 lattice intersections within the cube. This cube within the protein's active site is shown in figure 2. The centre of the cube was placed onto the point identified at the first step of the study as a position for the ACh carbonyl carbon atom. A bulky and very active organophosphorous inhibitor, the *S*-enantiomer of compound **2** was selected for the second step. Three criteria were taken into account when selecting

Table 1 Stereospecific AChE inhibitors with chiral phosphorous and inhibition constants for R- and S-enantiomers



Cmpd	R ₁ = X (leaving group)	R ₂	R ₃	K _I (M*min)×10 ⁴
1		-O-iso-propyl	methyl	S 5000
				R 4.1
2		-O-cyclopentyl	methyl	S 70000
				R 21
3		-O-iso-propyl	methyl	S 20000
				R NA
4		-S-butyl	methyl	S 5.5
				R 280
5			-O-iso-propyl	NA
6			methyl	NA

the phosphorous positions corresponding to the productive inhibitor-enzyme complex namely (i) the ligand-enzyme complex energy, (ii) the distance from the catalytic serine residue - we did not consider the most distant phosphorous positions - and (iii) the orientation of the phosphoryl group - the orientations towards the oxyanion hole were given a higher priority.

At the third step, the other inhibitors were docked to the enzyme. The position selected for the phosphorus atom at

the second step was used as the anchor point. The docking procedure was applied to these inhibitors in the same manner as it was applied to ACh at the first step but using the phosphorus atom instead of the quaternary nitrogen as the anchor point.

The lowest energy complexes obtained in the course of the automated docking procedure were optimised using the AMBER force field.

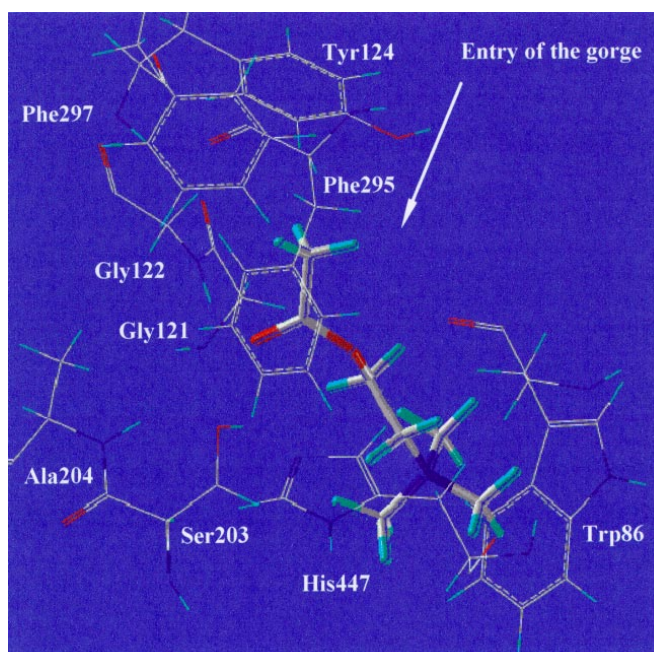


Figure 3 ACh docked to the catalytic site of MACHe

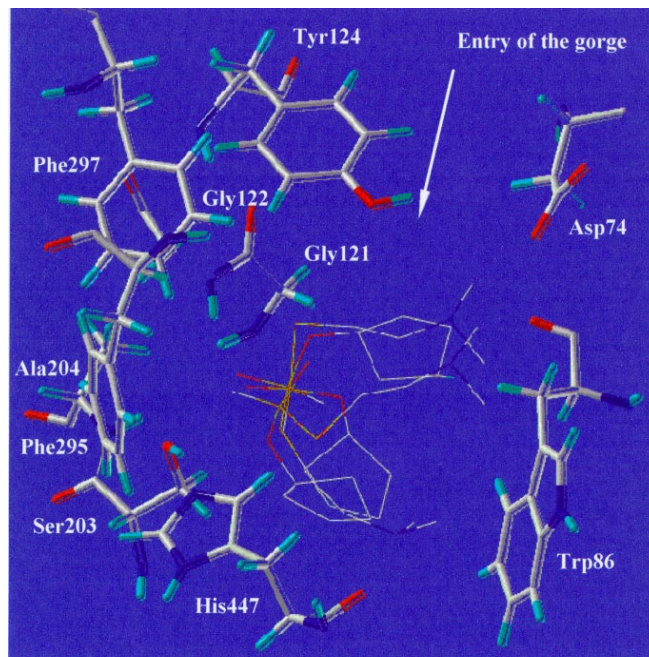


Figure 4 Three conformers found for the S-isomer of compound 2 which form low energy complexes within the catalytic site

Results

First step: Acetylcholine

The systematic docking of ACh revealed a number of low energy enzyme-ACh complexes. This result suggests that the enzyme possesses a rather spacious cavity which is able to bind the ACh molecule in various conformations and orientations. However we were interested in selecting a single structure of the substrate-enzyme complex which would serve as a model for the Michaelis complex whose formation precedes the acylation. A high turnover of the substrate indicates that the Michaelis complex is much more probable than any other. For a particular complex the probability of formation is determined by the entropy which is not taken into account in the molecular mechanics energy calculations. We used some external information in order to select the model of the Michaelis complex from the list of eight low energy complexes. The energy of complex formation could not serve as a reliable selection criterion because it varied within quite a narrow range, 4 kcal·mol⁻¹. Some recent crystallographic studies on AChE complexed with substrate analogues [20, 29] suggest that the ACh carbonyl group should be oriented towards the triad Gly121, Gly122 and Ala204, referred to as the "oxyanion hole" [30]. Only two of the eight low energy complexes had the ACh carbonyl group oriented towards the "oxyanion hole". The substrate geometries in these two com-

plexes were so similar that with the geometry optimisations both fell into the same energetic minimum. We considered this optimised structure shown in figure 3 as a model for the Michaelis complex and used the co-ordinates of the carbonyl carbon atom as a starting point for the second step of the docking analysis.

Second step: S-enantiomer of compound 2

Translation of the inhibitor's phosphoryl through the 125 lattice intersections near the catalytic serine, in combination with the re-orientation and torsion of rotatable bonds for the whole molecule, resulted in a number of reliable phosphorous atom positions, i.e. those positions which led to low-energy complexes. More particularly, 15 positions lying in a compact (1.5Å × 1Å × 0.5Å) region produced, for this inhibitor, three conformational families, i.e. groups of similar conformations whose orientation and torsion angles do not differ by more than 30°. The first family occupies 7 lattice intersections and has its phosphoryl group oxygen oriented towards the oxyanion hole (Gly121, Gly122, Ala204) and the quaternary nitrogen towards the entrance of the gorge (Asp74). The second family of conformers occupies 6 lattice intersections and differs from the first family by the position of the quaternary nitrogen which interacts with Trp86. The third family occupies 2 lattice intersections and has its phosphoryl group oxygen oriented away from the oxyanion hole. Figure

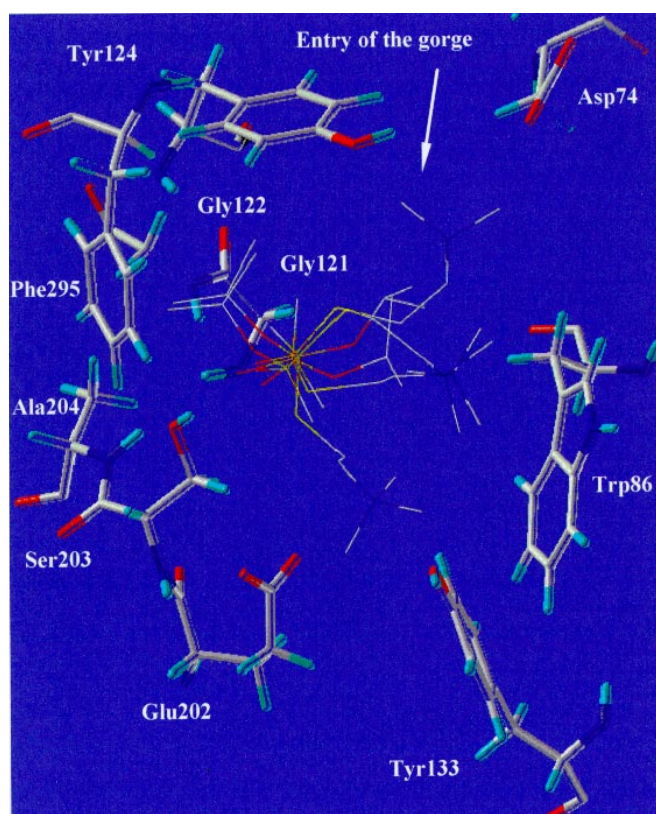


Figure 5 Four conformers found for the R-isomer of compound 1 which form low energy complexes within the catalytic site

4 shows lowest energy representatives for each family aligned according to their orientations within the enzyme cavity.

In order to define the lattice intersection and the inhibitor's conformer that lead to the most stable inhibitor-enzyme complex, we optimised the geometry for all the selected low energy complexes. In the first family, two conformers lead to two lowest energy complexes. Their complex formation energies (ΔE_c) (-55.90 and -53.70 kcal.mol⁻¹) are comparable and are substantially lower than those of the other members of the family. The phosphorus atoms of these two conformers are very close from each other (0.30 Å). The torsion angle differences that exist between the conformers in non-optimised structures were decreased in the course of optimisation. The high degree of similarity between these two conformers suggests that they lead to the same inhibitor-enzyme complex and the slight differences between them are only due to an inaccuracy inherent to the optimisation algorithm. For our further analyses, we selected a single structure leading to a slightly lower complex formation energy (-55.90 kcal.mol⁻¹).

In the second family, the choice was facilitated by the fact that the lowest energy complex (ΔE_c = -68.94 kcal.mol⁻¹) had an energy 15 kcal.mol⁻¹ lower than that of its nearest energetic neighbour. This significant difference allowed us

to select the corresponding conformer and phosphorus atom position for the next step of the study.

For the third family, the lowest energy complexes had energies 20-30 kcal.mol⁻¹ higher than those of the lowest energy members of the first and second families. Hence, no conformers were selected from this family.

The two conformers selected from the first and second families are rather different. One of them (ΔE_c = -55.88 kcal.mol⁻¹) has its cationic substituent oriented towards the entry of the gorge (Tyr337, Tyr121 and Asp 74) and its O-cyclopentyl group located in a hydrophobic cavity formed by residues Trp86, Tyr133, Ile451 and Glu202. The other (ΔE_c = -68.94 kcal.mol⁻¹) has its quaternary nitrogen interacting with the "anionic" site (Trp86). The probability of each of these two complexes existing will be discussed below in the context of the results obtained for the other inhibitors. At this stage, the most important issue is to define the phosphorus atom position as the anchor point for further docking analyses. From this point of view, the two pre-selected conformers are not too different, as their phosphorus atoms occupy the neighbouring lattice intersections. To reduce the computational time of further analyses, we chose a single anchor located at the middle point between these two lattice intersections. This makes an acceptable 0.25 Å deviation from each selected position, that equalises the chances for appearing conformers with the cationic group oriented towards either Trp86 or Trp286. The resulting anchor point is situated at 2.29 Å, 1.74 Å and 3.04 Å from the oxyanion hole triad (Gly121, Gly122, Ala204, respectively) and at 3.54 Å from the reacting Ser203.

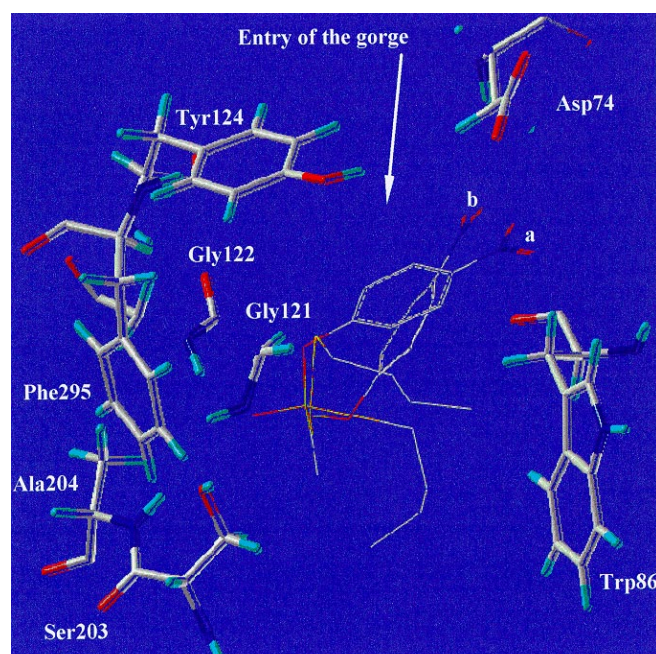


Figure 6 Low energy complexes obtained for (a) the R-isomer and (b) S-isomer of compound 4

Third step: Other inhibitors

Compound 1 - Docking the *S*-enantiomer of compound **1** resulted in three different low energy complexes. Two of these complexes have slightly lower energies than those of the complexes obtained by docking the *R*-enantiomer of the same inhibitor. The conformations and orientations of the inhibitor in these complexes are very similar to those in the two "best" complexes with the *S*-enantiomer of compound **2**. The complex formation energies are $-45.77 \text{ kcal}\cdot\text{mol}^{-1}$ for the complex with the inhibitor's quaternary nitrogen oriented towards Trp86 and $-44.74 \text{ kcal}\cdot\text{mol}^{-1}$ for the complex with this quaternary nitrogen oriented towards Asp74 and the methyl substituent oriented towards Phe295. The third conformer ($\Delta E_C = -33.05 \text{ kcal}\cdot\text{mol}^{-1}$) has its quaternary nitrogen interacting with Asp74 and the methyl substituent oriented towards Phe297.

Docking the *R*-enantiomer of compound **1** produced four different low energy complexes. The inhibitor in the lowest energy complex ($\Delta E_C = -42.60 \text{ kcal}\cdot\text{mol}^{-1}$) has its phosphoryl oxygen oriented towards the oxyanion hole, the quaternary nitrogen interacting with Trp86 and the methyl substituent oriented towards Phe297 and Tyr124. In three other complexes, the inhibitor's phosphoryl groups are similarly oriented but turned 60° around the P=O axis relatively to the phosphoryl's orientation in the lowest energy complex, as shown in figure 5. Of the three latter complexes, the most stable one ($\Delta E_C = -39.24 \text{ kcal}\cdot\text{mol}^{-1}$) has the inhibitor's quaternary nitrogen interacting with Trp86. The other two have the inhibitor quaternary nitrogens interacting with (i) Asp74 ($\Delta E_C = -29.41 \text{ kcal}\cdot\text{mol}^{-1}$) and (ii) Tyr133/Glu202 ($\Delta E_C = -23.03 \text{ kcal}\cdot\text{mol}^{-1}$).

Compound 2 - Two low energy complexes were found for the *R*-enantiomer of compound **2**. In the first complex ($\Delta E_C = -38.45 \text{ kcal}\cdot\text{mol}^{-1}$), the cyclopentyl group is directed towards the entry of the cavity. The cationic nitrogen is placed 3.3 \AA away from the Tyr133 hydroxyl and 4.2 \AA away from the Glu202 carboxyl group. Two attractive interactions probably stabilise this complex, namely an electrostatic interaction with Glu202 and a hydrogen bond between the Tyr133 hydroxyl oxygen and the hydrogen bonded to the cationic nitrogen. For the other conformer found ($\Delta E_C = -42.62 \text{ kcal}\cdot\text{mol}^{-1}$), the cyclopentyl group occupies the pocket formed by Ile451, Tyr133, Trp86 and Glu202 and the cationic group is oriented towards Trp86.

Compound 3 - This compound has a long cationic group. For the more active *S*-enantiomer we found two low energy complexes. Again, the phosphoryl group and substituents are oriented almost in the same way as those of the *S*-enantiomers of compounds **1** and **2**. The formation energy for the complex with the inhibitor's quaternary nitrogen interacting with Trp86 is $-44.68 \text{ kcal}\cdot\text{mol}^{-1}$. The formation energy of the second complex is $-39.53 \text{ kcal}\cdot\text{mol}^{-1}$ and the inhibitor's quaternary nitrogen is oriented towards Asp74. In both complexes, the inhibitor's long cationic substituent is folded.

The *R*-enantiomer forms the only low energy complex ($\Delta E_C = -30.54 \text{ kcal}\cdot\text{mol}^{-1}$) with the inhibitor's phosphoryl and methyl groups oriented in the same way as in the complex with the *S*-enantiomer, whose quaternary nitrogen is oriented towards Asp74. It was also found that the cationic substituent of the *R*-enantiomer does not have enough space to adopt the orientation towards Trp86.

Compound 4 - In contrast to the other compounds studied, compound **4** is not charged. Another particularity of this inhibitor is that its *R*-enantiomer has a higher inhibitory activity. Two low energy complexes were found for this *R*-enantiomer. The more stable complex ($\Delta E_C = -27.78 \text{ kcal}\cdot\text{mol}^{-1}$) has its leaving group oriented towards the entry of the gorge. The second complex has a formation energy of $-13.07 \text{ kcal}\cdot\text{mol}^{-1}$ and its leaving group is oriented towards Trp86.

For the *S*-enantiomer, our automated docking produced two low energy complexes. In both of them the inhibitor's phosphoryl and methyl groups are oriented similarly to those in the lowest energy complex of the *R*-enantiomer, as shown in figure 6. Hence, the breaking bond P-O is oriented differently than that of more active *R*-enantiomer. The leaving nitrophenyl is oriented towards Asp74 in the lower energy complex ($\Delta E_C = -26.51 \text{ kcal}\cdot\text{mol}^{-1}$) and towards Trp86 in the other.

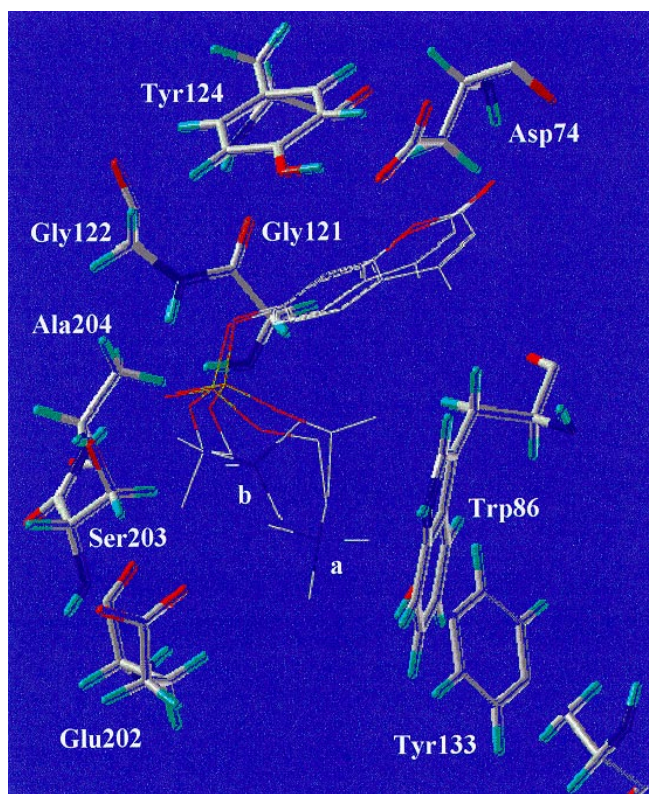


Figure 7 Low energy complexes obtained for (a) the *R*-isomer and (b) *S*-isomer of compound **5**

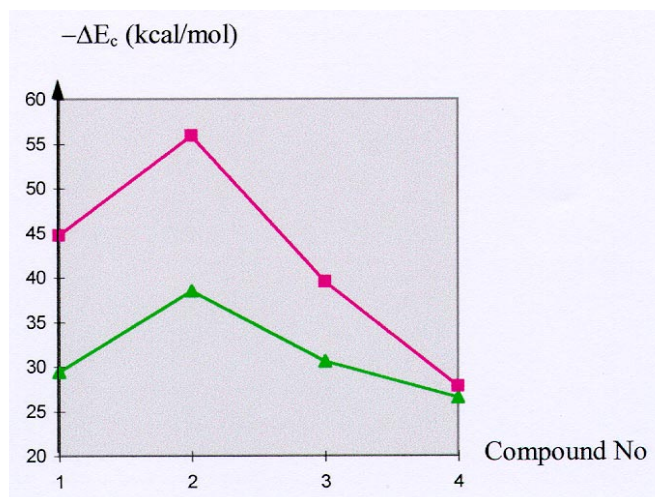


Figure 8 Complexation energies for more active isomers (squares) and less active isomers (triangles) of compounds 1-4

Compound 5 - For this inhibitor, the docking analysis yielded unambiguous results. Two low energy complexes (one per enantiomer) were found and their alignment is shown in figure 7. The corresponding complex formation energies are $-58.64 \text{ kcal}\cdot\text{mol}^{-1}$ for the *S*-enantiomer and $-55.39 \text{ kcal}\cdot\text{mol}^{-1}$ for the *R*-enantiomer. In both complexes the leaving coumarinyl group is oriented towards the entry of the gorge. It probably has favourable interactions with a triad of the side chains belonging to Asp74, Tyr124 and Tyr337. The cationic substituent has different spatial arrangements in these two complexes. The quaternary nitrogen of the *S*-enantiomer interacts with Trp86, while the quaternary nitrogen of the *R*-enantiomer is oriented towards and probably interacts with Tyr133 and Glu202.

Compound 6 - Two low energy complexes were found for the *S*-enantiomer of this inhibitor. The inhibitor in the lower energy complex ($\Delta E_c = -54.87 \text{ kcal}\cdot\text{mol}^{-1}$) has similar geometry and orientation as those observed in the unique complex of the *S*-enantiomer of compound 5, i.e. the coumarinyl substituent is oriented towards the entry of the gorge and the quaternary nitrogen interacts with Trp86. The inhibitor in the higher energy complex ($\Delta E_c = -52.61 \text{ kcal}\cdot\text{mol}^{-1}$) has the same geometry as in the low energy complex but its orientation is different. The higher energy complex can be obtained from the lower energy one by turning it 120° around the P=O axis.

The inhibitor's geometry inside the lowest energy complex found for the *R*-enantiomer ($\Delta E_c = -60.36 \text{ kcal}\cdot\text{mol}^{-1}$) mimics that inside the unique complex obtained for the *R*-enantiomer of compound 5. Again, as in the case of the *S*-enantiomer, the second low energy complex for the *R*-enantiomer ($\Delta E_c = -40.63 \text{ kcal}\cdot\text{mol}^{-1}$) can be obtained from the first one by turning it 120° around the P=O axis.

Discussion

The first clear result of this study concerns the orientation of the phosphoryl group. For every compound studied, the orientation of the phosphoryl's oxygen towards the oxyanion hole was more energetically favourable than the opposite direction.

A second point concerns the orientation of the leaving group. We attempted to construct a model of the productive Michaelis complex which would explain the difference in activity between *S*- and *R*-enantiomers. At present, there are two major hypotheses on how the leaving group is located within this complex. The first trivial one supposes the leaving group occupies approximately the same position as the leaving group of the substrate does, i.e. oriented towards Trp86. The second hypothesis recently advanced by Hosea *et al* [1] and also supported by Albaret *et al.* [23] suggests that the thiocholine leaving group of organophosphate inhibitors is oriented towards Asp74. According to Hosea *et al.*, this orientation represents "a productive configuration allowing for facile direct in-line attack by the γ -oxygen of Ser203 and easy displacement of the thioate moiety".

With respect to these two hypotheses our inhibitors can be classified into two groups. The first group includes the *R*- and *S*-enantiomers of compounds 1, 2 possessing a thiocholinyl leaving group. For the more active *S*-enantiomers of these two inhibitors, low energy complexes satisfying both hypoth-

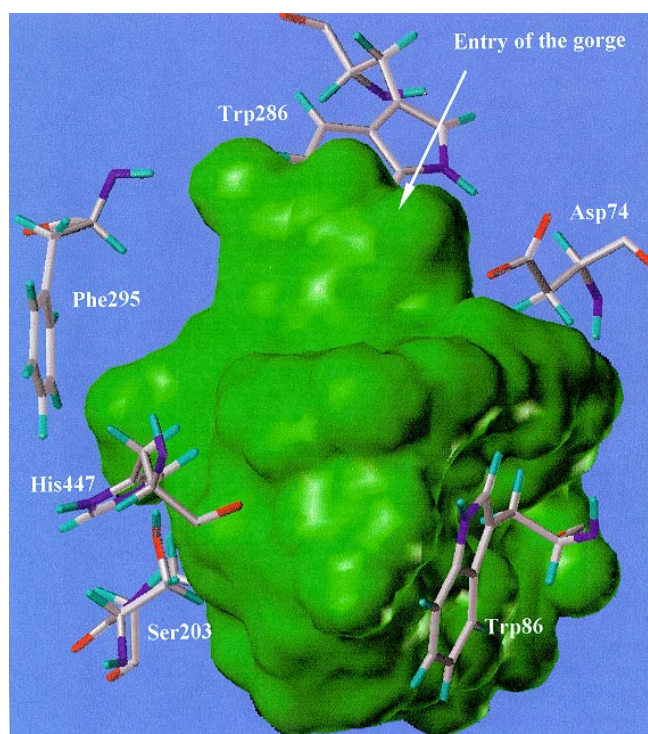


Figure 9 Complete accessible volume within the catalytic site of MACH E resulting from the alignment of irreversible inhibitors

eses were isolated in the course of our docking study. In the first type of complexes, the cationic group is oriented towards the entry of the gorge, the O-alkyl substituent is received within the hydrophobic region formed by Ile451, Tyr133, Glu202, while the methyl group is oriented towards His447. In the second type of complexes, the cationic group interacts with Trp86, the O-alkyl group is oriented towards residues Tyr124, Phe297 at the entry of the gorge and the methyl group occupies the pocket formed by Ile451, Tyr133 and Glu202.

The *R*-enantiomers of compounds possessing a thiocholy leaving group can easily adopt such a position within the cavity when this group interacts with Trp86, while the orientation of the leaving group towards Asp74 is less accessible to them. Instead of taking this direction the leaving group takes the intermediate one towards residues Tyr133, Glu202.

The equal facility for *R*- and *S*-enantiomers to form the inhibitor-protein complex with the inhibitor's thiocholy leaving group interacting with Trp86 leads us to suppose that this type of complexes is non-productive. Indeed, much less active *R*-enantiomers should not normally so easily form the Michaelis complex. This is the case for the second type of complexes, where the *S*-enantiomers easily place the thiocholy group in the direction of Asp74 allowing an effective in-line attack by the γ -oxygen of Ser203, while *R*-enantiomers have their breaking P-S bond slightly disoriented from the ideal direction allowing the in-line attack. This disorientation is probably a reason for the lower inhibitory activity.

The second group contains compounds 4-6 that have more sterically constrained aromatic leaving groups. For these inhibitors, there is not enough room to orient the aromatic leav-

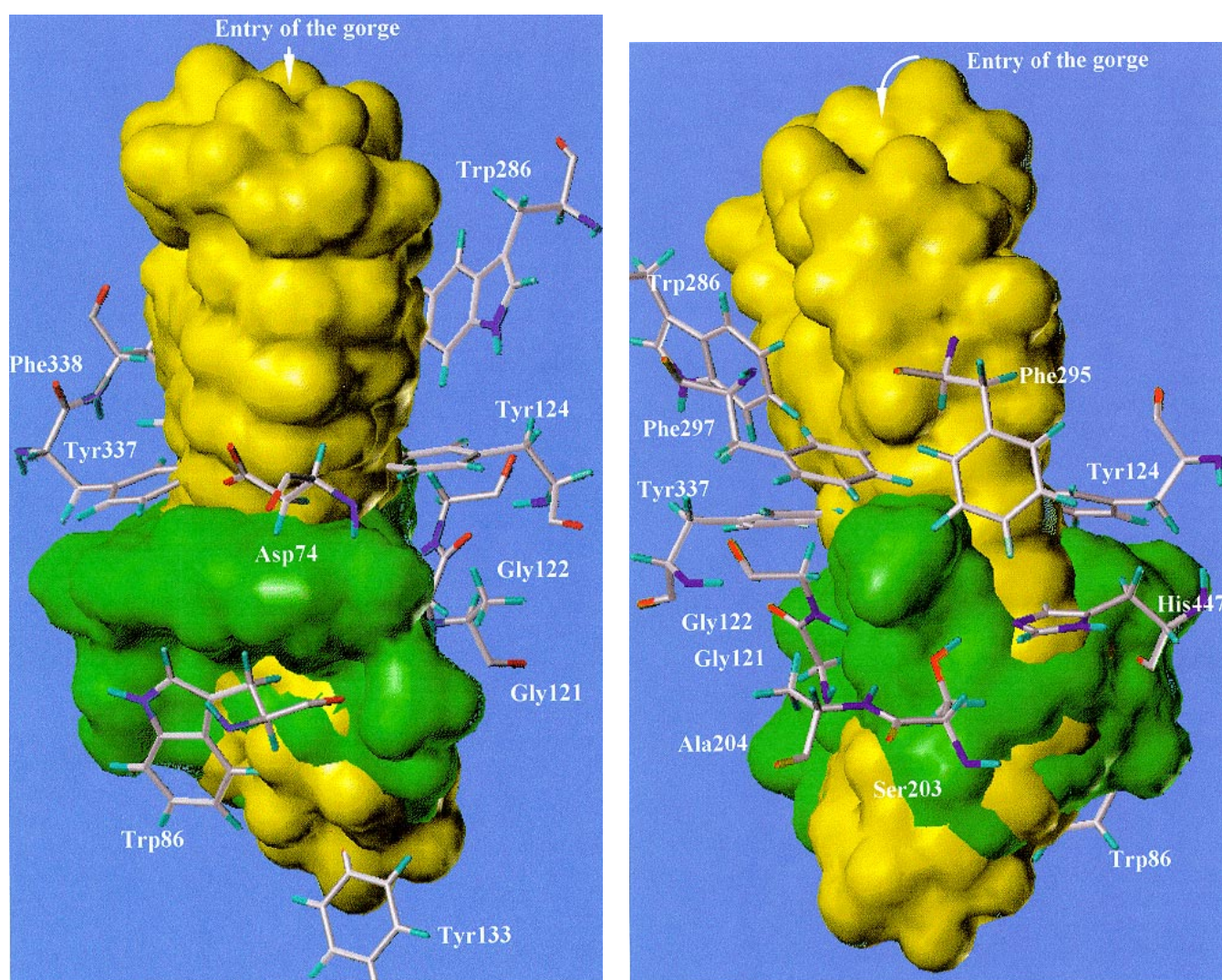


Figure 10 Complete accessible volume within the active site of MACHe resulting from the alignment of reversible (yellow) and irreversible (green) inhibitors, (a) view from the anionic subsite side, (b) view from the esterase subsite side

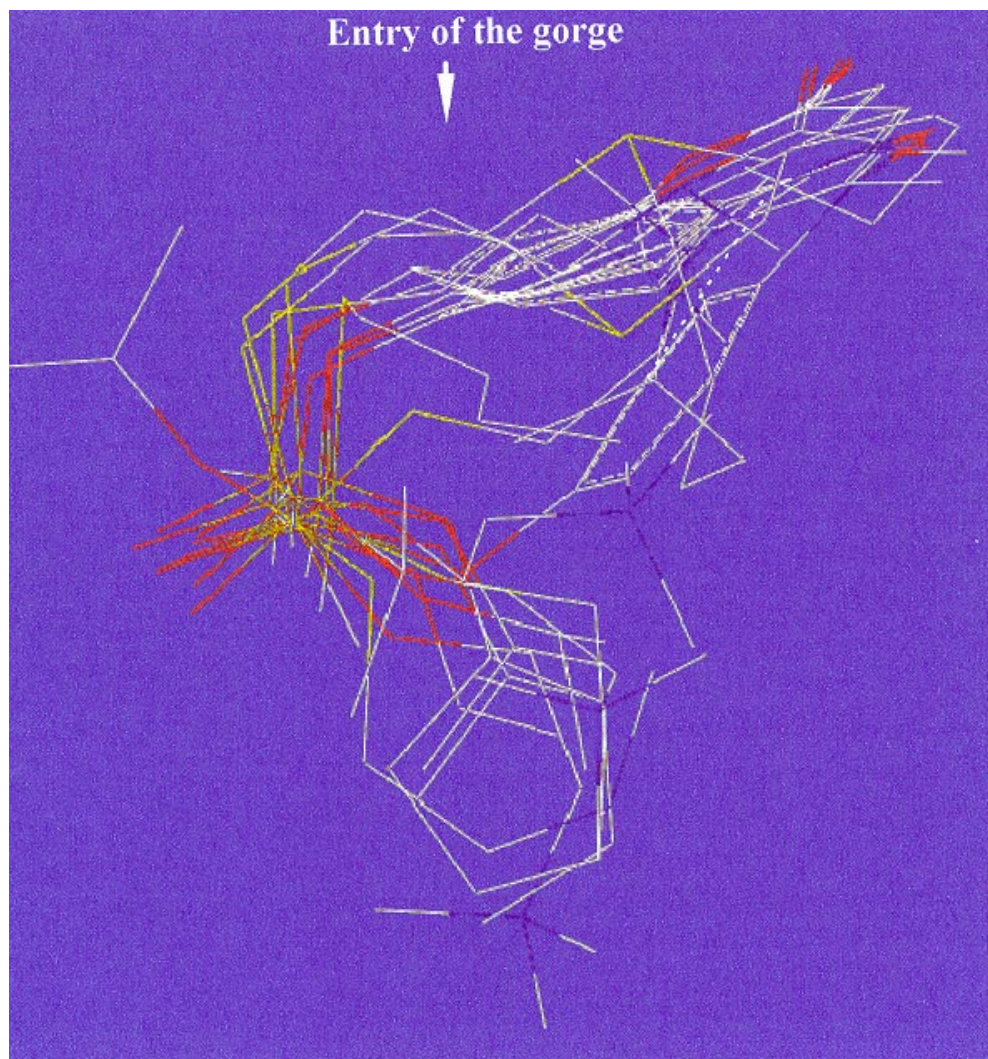
ing group towards Trp86. The models of the Michaelis complex obtained for these compounds allow us to explain the difference between more and less active enantiomers. For example, the P-S bond of the less active *S*-enantiomer of compound 4 cannot take an ideal orientation allowing an effective in-line attack since the thiobutyl group cannot fit the pocket formed by His447, Phe295 and Phe297 because of the steric hindrance.

An important question arising after identifying a new potent inhibitor is which of its two enantiomers is the more active. An essential parameter helping to answer this question is the inhibitor-enzyme interaction energy. The more active enantiomer should fit the active site better. The diagram in figure 8 shows the differences between the energies obtained for more active and less active enantiomers. For all three inhibitors whose activity was measured separately for each enantiomer, the interaction energy of the more active enantiomer is lower than the energy obtained for the less active one. Moreover, the difference in energy between more active and less active enantiomers is proportional to their activity difference.

The inhibitor structures when extracted from the models of the Michaelis complex obtained in this study constitute a specific alignment which may be used for calculating CoMFA [31] fields and establishing a CoMFA model. Such a type of alignment referred to as "natural" was successfully applied to a series of reversible AChE inhibitors in our previous study [22]. The same approach can be used further to establish a three dimensional QSAR model for the organophosphorous inhibitors.

Finally, our study delineated the three-dimensional geometry of the cavity available to the irreversible AChE inhibitors at the active site of the enzyme. Unlike the previous approaches to describe the active site, which could be referred to as protein-based approaches, this one is inhibitor-based. Indeed, the previous studies of the AChE active site exploited site-specific mutagenesis based firstly on the knowledge of the enzyme's primary structure and then on its three-dimensional structure [1, 10, 13, 20]. These studies resulted in a simple and reliable model of the active site consisting of the anionic and esterase subsites which together form the catalytic site and the peripheral anionic site. Additionally, an

Figure 11 Naturally aligned structures of organophosphorous inhibitors extracted from the productive enzyme-ligand complexes obtained by automated docking



"acyl pocket" receiving either the acyl group of the substrate or the small non-leaving group of the organophosphorous compounds [21] was recently described. This modular model of the active site advanced the design of new inhibitors. However, this degree of simplification does not always allow us to explain or to predict the activity of a new inhibitor.

In our studies, we used the inhibitors as probes in order to obtain a mould of the space available to a ligand within the enzyme. In the course of our automated docking, we collected hundreds of low energy complexes with different inhibitors. Not all these complexes are necessarily productive, but the purpose of this part of our study was to probe a possibly large portion of the sterically available space. Figure 9 shows the volume obtained by superposition of all the organophosphorous inhibitors studied extracted from the low energy complexes that were studied. Figure 10 shows the combined volume obtained by probing the cavity with organophosphorous inhibitors and with reversible inhibitors whose docking was reported in our previous paper [22]. The volumes shown in figures 9 and 10 illustrate the fact that the cavity within the enzyme has smooth surface and does not consist of easily distinguishable pockets. These moulds could be helpful in constructing a specific inhibitor which would have structural features of both reversible and irreversible inhibitors. Figure 11 shows that the location of the inhibitors' most important functional groups, e.g. the phosphoryl group or the quaternary nitrogen, within the enzyme can widely vary depending on the shape and volume of the other groups in the molecule and on the chirality of the phosphorus atom. On the other hand, for different inhibitors there are some regularities among the complexes obtained. For example, the aromatic leaving groups lie practically in the same plane and are probably stabilised by interactions with Tyr124 and Tyr341. The quaternary nitrogen atoms or the tertiary sulphur atoms belonging to the cationic leaving group are located close to the centre of the aforementioned plane of the aromatic leaving group. The most probable stabilising factor in this case is an electrostatic interaction of the cation with Asp74.

Conclusion

Our automated docking for a series of *S*- and *R*-enantiomers of 6 organophosphorous irreversible inhibitors of acetylcholinesterase suggests that the leaving group in the Michaelis complex is directed towards the entry of the active site (Asp74). This orientation supports an effective in-line attack of the phosphorus atom, as it was recently suggested by Hosea *et al* [1].

The totality of low energy complexes obtained in the course of the automated docking study allowed to create a three-dimensional model of the catalytic cavity available to various organophosphorous compounds within the active site. We have not taken in this approach, in first approximation, the potent contribution and/or of perturbation of water molecules in the interaction process ligand/AChE. Work is

underway to study this point on model compounds with molecular dynamics.

The structures of docked inhibitors constitute a "natural" alignment which is being currently used to establish three dimensional quantitative structure-activity relationships by CoMFA in support of the computer-aided molecular design of organophosphorous antidote compounds.

References

- Hosea, N.A.; Radic, Z.; Tsigelny, I.; Berman, H.A.; Quinn, D.M.; Taylor, P. *Biochemistry* **1996**, *35*, 10995-11004.
- Nachmansohn, D. *Proc. Natl. Acad. Sci. U. S.* **1968**, *61*, 1034-1041.
- (a) Villalobos, A.; Blake, J. F.; Biggers C. K.; Butler, T. W.; Chapin, D. S.; Chen, Y.L.; Ives, J. L.; Jones, S. B.; Liston, D. R.; Nagel, A. A.; Nason, D. M.; Nielsen, J. A.; Shalaby, I. A.; Frost White, W. *J. Med. Chem.* **1994**, *37*, 2721-2734. (b) Sugimoto, H.; Iimura, Y.; Yamanishi, Y.; Yamatsu, K. *Bioorg. & Med. Chem. Lett.* **1992**, *2*, 871-876.
- Sugimoto, H.; Tsuchiya, T.; Sugumi, H.; Higurashi, K.; Karibe, N.; Iimura, Y.; Sasaki, A.; Kawakami, Y.; Araki, S.; Yamanishi, Y.; Yamatsu, K. *J. Med. Chem.* **1992**, *35*, 4542-4548.
- Sanborn, J.R.; Fukuto, T.R. *J. Agr. Food Chem.* **1972**, *20*, 926-930.
- Froede, H.C.; Wilson, I.B. in *The enzymes*, Boyer P.D., Ed., Academic Press, New York, 3rd ed., **1971**, *5*, 87-114.
- Aldridge, W.N.; Reiner E. in *Enzyme inhibitors as substrates*, North Holland Publishing Co., Amsterdam, **1972**.
- Ariëns, E.J.; van Rensen, J.J.S.; Welling, W. (Editors), *Stereoselectivity of pesticides; biological and chemical problems*, Elsevier Science Publishers B. V., Amsterdam, **1988**.
- Berman, H.A.; Leonard, K. *J. Biol. Chem.* **1989**, *29*, 3942-3950.
- Brestkin, A.P.; Godovikov N.N. *Russian Chemical Reviews* **1978**, *47*, 859-869.
- Gupta, S.P.; Singh, P.; Bindal M.C.; *Indian J. Chem.*, **1979**, *17B*, 605-609.
- Ashman, W.P.; Groth M.J. Structure toxicity relationships of methylphosphonofluoridate analogues. Proceedings of the scientific conference on chemical and biological defense, **1995**.
- Järv, J. *Bioorg. Chem.* **1984**, *12*, 259-278.
- Nachmansohn, D.; Wilson, I.B. *Adv. Enzymol.* **1951**, *12*, 259-339.
- Bergmann, F.; Wilson I.B.; Nachmansohn D. *Biochim. Biophys. Acta* **1950**, *6*, 217-224.
- Ordentlich, A.; Barak, D.; Kronman, C.; Ariel, N.; Segall, Y.; Velan, B.; Shafferman, A., *J. Biol. Chem.* **1996**, *271*, 11953-11962.
- Sussman, J. L.; Harel, M.; Frolow, F.; Oefner, C.; Goldman, A.; Toker, L. ; Silman, I. *Science* **1991**, *253*, 872-879.

18. Bourne, Y.; Taylor, P.; Marchot, P. *Cell* **1995**, *83*, 503-512.
19. Radic, Z.; Pickering, N.A.; Vellom, D.C.; Camp, Sh.; Taylor, P. *Biochemistry* **1993**, *32*, 12074-12084.
20. Ordentlich, A.; Barak, D.; Kronman, Ch.; Flashner, Y.; Leitner, M.; Segal, Y.; Ariel, N.; Cohen, S.; Velan, B.; Shafferman, A. *J. Biol. Chem.* **1993**, *268*, 17083-17095.
21. Hosea, N.A.; Bermann, H.A.; Taylor, P. *Biochemistry* **1995**, *34*, 11528-11536.
22. Bernard, P.; Kireev, D.B.; Chretien, J.R.; Fortier, P.L.; Coppet, L. *J. Comput.-Aided Mol. Des.* **1998**, in press.
23. Albaret, C.; Lacouture, S.; Ashman, W.P.; Froment, D.; Fortier, P.L. *Proteins: Struct., funct. and Genet.* **1997**, *28*, 543-554.
24. Sybyl 6.3 available from Tripos Associates, 1699 South Hanley Road, St Louis, MO 63144.
25. Weiner, S.J.; Kollman P.A.; Nguyen, D.T.; Case D.A. *J. Comp. Chemistry* **1986**, *7*, 230-252.
26. Harel, M.; Schalk, I.; Ehret-Sabatier, L.; Bouet, F.; Goeldner, M.; Hirth, C.; Axelsen, P.; Silman, I.; Sussman, J. L. *Proc. Natl. Acad. Sci.* **1993**, *90*, 9031-9035.
27. Dougherty, D. A.. *Science* **1996**, *271*, 163-168.
28. Clarc, M.; Cramer, R.D.III; Opdenbosch, N.V. *J. Comput. Chem.* **1989**, *10*, 982-1012.
29. Harel, M.; Quinn, D.M.; Nair, H.K.; Silman, I.; Sussman, J.L. *J. Am. Chem. Soc.* **1996**, *118*, 2340-2346.
30. Steitz, T.A.; Shulman, R.G. *Annu. Rev. Biophys. Bioeng.* **1982**, *11*, 419-444.
31. Cramer, R. D. III; Patterson, D. E.; Bunce, J. D. *J. Amer. Chem. Soc.* **1988**, *110*, 5959-5967.